Journal Pre-proof

Influence of SO_4^{2-} anionic group substitution on the enhanced photoluminescence behaviour of red emitting $CaMoO_4:Eu^{3+}$ phosphor

M.L.A. Letswalo, L. Reddy, A. Balakrishna, H.C. Swart, O.M. Ntwaeaborwa

PII: S0925-8388(20)33386-7

DOI: https://doi.org/10.1016/j.jallcom.2020.157022

Reference: JALCOM 157022

To appear in: *Journal of Alloys and Compounds*

Received Date: 21 June 2020

Revised Date: 31 August 2020

Accepted Date: 2 September 2020

Please cite this article as: M.L.A. Letswalo, L. Reddy, A. Balakrishna, H.C. Swart, O.M. Ntwaeaborwa, Influence of SO_4^{2-} anionic group substitution on the enhanced photoluminescence behaviour of red emitting $CaMoO_4:Eu^{3+}$ phosphor, *Journal of Alloys and Compounds* (2020), doi: https://doi.org/10.1016/j.jallcom.2020.157022.

This is a PDF file of an article that has undergone enhancements after acceptance, such as the addition of a cover page and metadata, and formatting for readability, but it is not yet the definitive version of record. This version will undergo additional copyediting, typesetting and review before it is published in its final form, but we are providing this version to give early visibility of the article. Please note that, during the production process, errors may be discovered which could affect the content, and all legal disclaimers that apply to the journal pertain.

© 2020 Published by Elsevier B.V.

Journal Pre-proof

Sample CRediT author statement

M.L.A Letswalo: Writing - Original Draft**,** Conceptualization, Methodology, Software

L. Reddy: Resource, Data curation, Funding acquisition.

A. Balakrishna: Software, Validation, Conceptualization, Writing - Review & Editing

H.C. Swart: Resource, Conceptualization, Writing - Review & Editing

O.M. Ntwaeaborwa: Resource, Validation, Conceptualization, Visualization Writing - Review & Editing **&** Supervision

Journal Pre-proof

Graphical abstract:

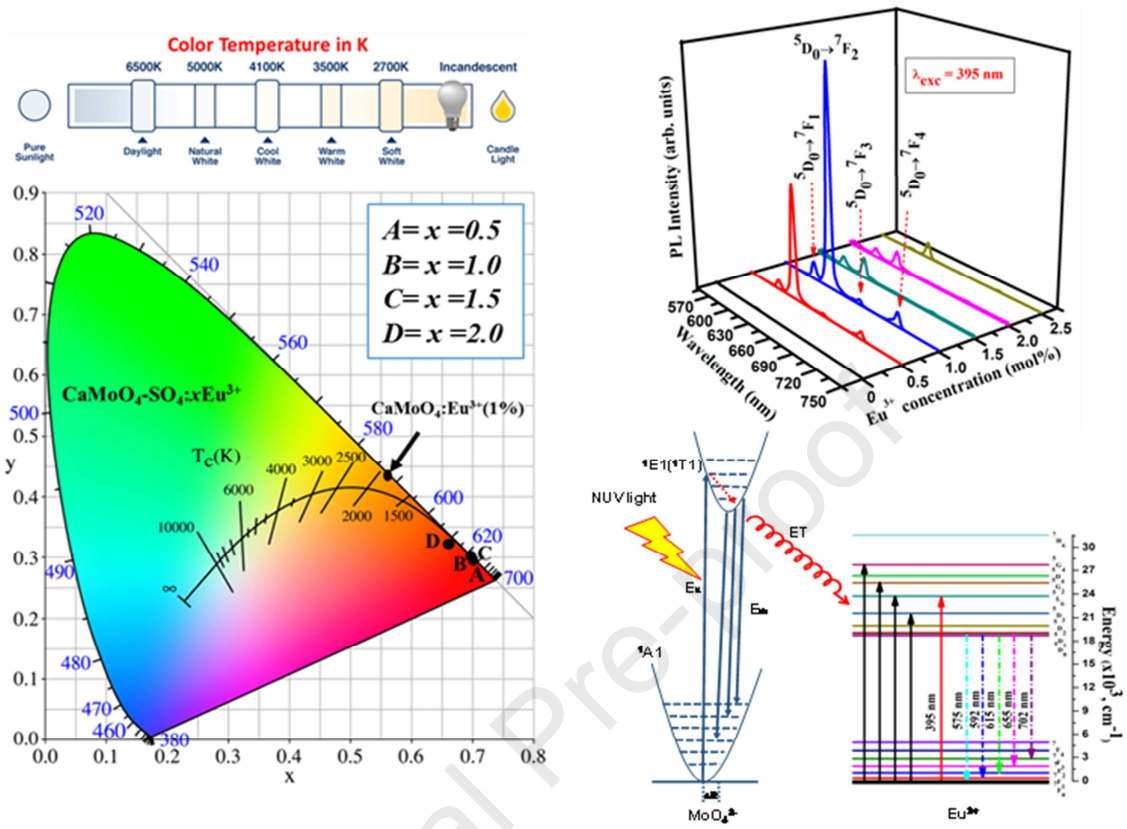

Journal Pre-proof

Journal Pre-proof

Influence of SO_4^{2-} anionic group substitution on the enhanced photoluminescence behaviour of red emitting $CaMoO_4:Eu^{3+}$ phosphor

M.L.A Letswalo[1*], L. Reddy[1], A. Balakrishna[1*], H.C. Swart[2] and O.M. Ntwaeaborwa[1*]

[1]*Department of Physics, University of Johannesburg, Johannesburg, ZA 2006, South Africa*

[2]*Department of Physics, University of the Free State, Bloemfontein, ZA 9300, South Africa*

Abstract

$CaMoO_4:xEu^{3+}$(x = 0.5, 1.0, 1.5, 2.0, and 2.5) powder phosphors incorporating SO_4^{2-} anions were synthesized at high temperature using the solid-state reaction technique. The structural, morphological and optical properties of these phosphors were analyzed using X-ray diffraction (XRD), field emission scanning electron microscopy, X-ray photoelectron spectroscopy, Fourier transform infrared spectroscopy and optical spectroscopy. The XRD results indicate that the incorporation of SO_4^{2-} anions and Eu^{3+} dopant ions did not affect the crystal structure of the $CaMoO_4$, but largely influenced the luminescence properties of the $CaMoO_4$-$SO_4:Eu^{3+}$ phosphors.The optical properties of our materials were examined using the UV-vis absorption spectroscopy. The absorption edges of the phosphors with different concentrations of Eu^{3+} were less than the band gap energy of the $CaMoO_4$ and their values ranged from 3.30 to 4.75 eV. The intensity of the red photoluminescence (PL) from $CaMoO_4:Eu^{3+}$ phosphors was enhanced considerably upon incorporation of SO_4^{2-} anions, suggesting that SO_4^{2-} acted to capture primary excitation energy and transfer it non-radiatively to Eu^{3+} ions. In addition, the incorporation of SO_4^{2-} ions also improved the fluorescence decay life-time values of the $CaMoO_4:xEu^{3+}$ phosphors significantly. Tunable emission was observed when the Eu^{3+} concentration was varied. Our PL results indicated that the $CaMoO_4$-$SO_4:Eu^{3+}$ phosphor exhibited the highest red emission intensity compared to $CaMoO_4$: Eu^{3+} phosphors, suggesting that $CaMoO_4$-$SO_4:Eu^{3+}$ could be a promising red component material for potential application in white light-emitting diode devices.

Keywords: solid-state reaction, $CaMoO_4$phosphors, SO_4^{2-} anionic group systems, Eu^{3+} ion, photoluminescence and white light-emitting diode (W-LEDs)

*Corresponding Authors: E-mail, leanyatsa.abram@gmail.com, bavula@uj.ac.za and ntwaeab@gmail.com

1. Introduction:

Nowadays, host materials with good thermal and chemical stability [1–5], excellent optical properties, and ease of incorporation of dopant ions are widely used to prepare phosphors for lighting applications. In particular, phosphors that are used for solid state lighting (SSL) applications in white light-emitting diodes (WLEDs). As a result, attention has been focused on improving the efficiency and lifetime of these phosphors. Although W-LEDs have been found to have high efficacy, relatively longer excited state life times, high energy efficiency and high color stability; the quality of white light is low due to a lower colour rendering index (CRI) and higher correlated colour temperature (CCT) due to deficiency of the red light component in commercial tricolor LEDs[6-11]. This study was therefore aimed at developing advanced red phosphor with high CRI and relatively low CCT that could be used as a source of red light, which will in turn improve the quality of white light output in tri-colour LEDs. Thus, this study was set out to prepare and evaluate fundamental properties of red light emitting phosphors for such practical application.

Due to their excellent optical and electromagnetic properties, and chemical stability, molybdate compounds are attractive host lattices for rare-earths (REs) dopant ions to prepare chemically stable phosphors that could be used in applications such as display technology, solid state lighting, Raman lasers, optical communication systems, and chemical catalysis[13,14]. Molybdates have therefore been investigated in different fields of research including production of advanced light emitting materials. In particular, the sheelite calcium molybdate is widely used as host for REs to prepare different types of phosphors. The sheelite structure of $CaMoO_4$ is composed of CaO_8 polyhedral and MoO_4 tetrahedron building blocks. The central Ca atom or Mo atom are properly aligned and are coordinated with eight or four O atoms, resulting in $CaMoO_4$ exhibiting compositional stability [15]. Moreover, $CaMoO_4$ has a broad higher absorption band range in the high energy region (i.e. ultraviolet or UV region), and can preferably emit high intensity blue or green light under UV excitation. When RE^{3+} ions are incorporated in the $CaMoO_4$ matrix and the material is excited by high energy photons, the captured primary excitation energy is transferred from the MoO_4^{2-} to the RE^{3+} ions, resulting in a dramatic increase in photoemission from the RE^{3+} ions [16]. In this study, we prepared red light emitting phosphor by doping $CaMoO_4$ with Eu^{3+}. In addition, we incorporated SO_4^{2-} anion group and we observed considerable improvement in the PL intensity of red emission from Eu^{3+} ions due to non radiative energy transfer from SO_4^{2-} and MoO_4^{2-} to the Eu^{3+} ions. Phosphors prepared from Eu^{3+} complexes

are used more often as sources of red light in a variety of displays and LEDs. These phosphors exhibit higher luminescence efficiency compared to other red light emitting materials [17] and they are being investigated by many researchers worldwide. For example, John Peteret.al.[18] investigated the PL properties of $CaMoO_4:Eu^{3+}$ (0.1 mol%) excited using near-UV radiation, and they observed a strong emission at 615 nm which was due to the forced electric dipole transitions $^5D_0 \rightarrow {}^7F_2$, which resulted in increased research interest in order to fully understand the luminescence behavior of Eu^{3+} in the $CaMoO_4$ host. However, the relatively low brightness and efficiency of $CaMoO_4:Eu^{3+}$ is not sufficient for application in commercial W-LEDs. Therefore, it is necessary to conduct further research to find away to enhance red emission from Eu^{3+} in the $CaMoO_4$ host. An investigation carried out by Wang et al. [19, 20] in which Eu^{3+} was co-doped with Bi^{3+} and Sm^{3+} showed an enhancement of the PL intensity of the Eu^{3+} ion. Recently, several studies have been conducted in which anions where used to substitute Mo^{6+} in the $CaMoO_4$ lattice sites. For example, a study carried out by Zhang et al. [21] showed an improvement in the red PL emission intensity of $NaEu(MoO_4)_2$ phosphor due to the incorporation of different anionic group systems. Furthermore, an enhanced red emission was observed from $NaLa(MoO_4)_2:Eu^{3+}$ due to the incorporation of SO_4^{2-} and BO_3^{3-} anionic groups[22]. In this study, SO_4^{2-} anions, which substituted MoO_4^{2-} sites in $CaMoO_4$ were found to enhance the intensity of red emission from $CaMoO_4:Eu^{3+}$. In addition, the effect of varying Eu^{3+} concentration on the intensity of the red PL emission was also investigated.

$CaMoO_4$-SO_4:$x$$Eu^{3+}$ (x = 0.5, 1, 1.5, 2, 2.5 mol. %) phosphor materials were synthesized via the solid state reaction route. SO_4^{2-} was incorporated into the MoO_4^{2-}sites resulting in enhanced red PL due to energy transfer from SO_4^{2-} to Eu^{3+}.We examined the structure, morphological, and optical properties of the $CaMoO_4$-SO_4:$x$$Eu^{3+}$ phosphors. A mechanism that explains the radiative transition is also discussed.

2. Experimental Procedure:

$CaMoO_4$-SO_4:xEu^{3+} (x = 0.5, 1.0, 1.5, 2.0, and 2.5) phosphors were prepared from highly pure chemical compounds, namely $CaCO_3$ (99.9% Sigma-Aldrich), MoO_3 (99.9% Sigma-Aldrich), $(NH_4)_2SO_4$ (99.9% Sigma-Aldrich) and Eu_2O_3 (99.99% Sigma-Aldrich). Stoichiometric amounts of the starting materials were mixed together in acetone using an agate mortar and pestle. The mixture was calcined at 1100 ^{0}C for 4 hours. The final mixture

was ground thoroughly using an agate mortar and pestle. The chemical reaction for the synthesis is given by:

$$CaCO_3 + MoO_3 + (NH_4)_2HSO_4 + Eu_2O_3 \rightarrow CaMoO_4SO_4Eu_2 + CO_2 + H_2O + 7H_2 + 2N_2 \quad (1),$$

and the schematic representation of the synthesis procedure is given by:

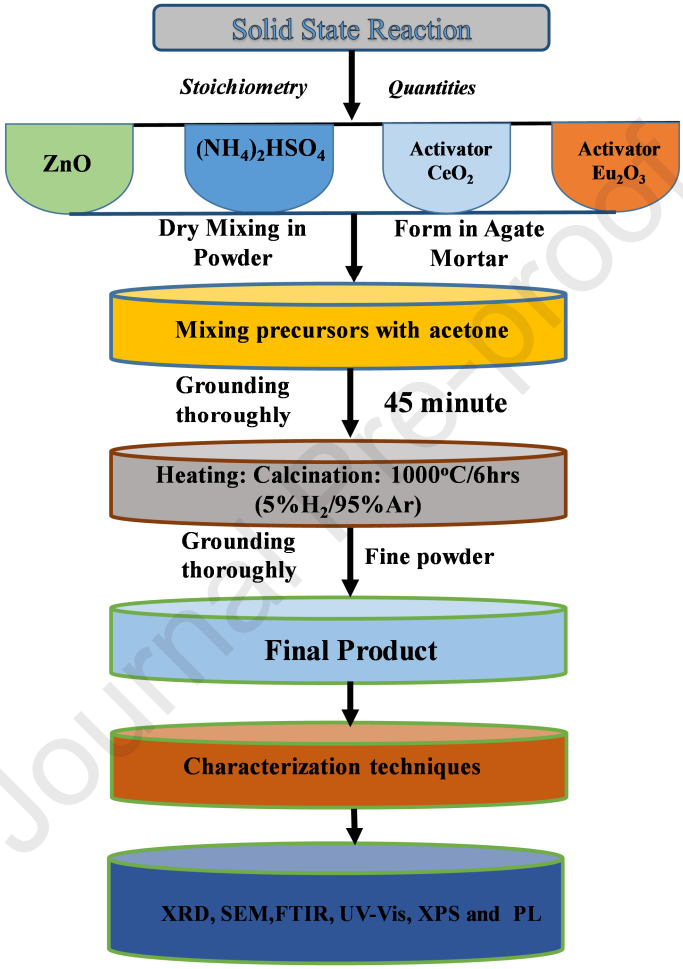

Fig. 1: *Schematic illustration of the sample preparation by the conventional solid-state reaction route.*

2.1 Characterization techniques:

Various techniques were used to characterize the samples. The crystal structure was analysed using X-ray powder diffraction (XRD) using a Bruker AXS D8 X-ray diffractometer with Cuk_{α} (1.5406Å). The data were recorded in 2θ range from 10^0 to 80^0. The particle morphology and the chemical composition were examined using a field emission scanning electron microscopy (FE-SEM) coupled with an Oxford Aztec 350 X-Max80 energy-

dispersive X-ray spectroscopy (EDS). The ultraviolet visible (UV-Vis) reflectance spectra were measured using a Perkin Elmer Lambda 950 spectrophotometer. Fourier transform infrared spectra (FTIR) were recorded using a Nicolet 6700 FTIR spectrometer in the spectral range of 4000– 400 cm^{-1}. The PL and the lifetime measurements were recorded in the fluorescence mode using the Cary eclipse spectrofluorometer using a 150W monochromatized xenon lamp as the excitation source. All characterizations were measured at room temperature.

3. Results and Discussion

3.1 Powder X-Ray diffraction analysis:

Fig 2 (a) shows the XRD profiles of $CaMoO_4$ and $CaMoO_4$-SO_4:xEu^{3+} (x = 0.5, 1.0, 1.5, 2.0 and 2.5 mol. %) measured in the range of 10-80°. All the diffraction peaks resemble those of the standard scheelite tetragonal structure of $CaMoO_4$. The peaks were indexed according to a standard XRD spectrum referenced in JCPDS file no. 29-351[23] of a pure tetragonal phase of $CaMoO_4$. The crystal structure as determined using the diamond software confirmed that our materials resemble the scheelite structure of $CaMoO_4$ with space group I41/a (no.88) as shown in Fig. 2(b). The crystal structure showsCa^{2+} and MoO_4^{2-} ionic sites, which can be occupied by Eu^{3+} and SO_4^{2-} ions, respectively, as reported elsewhere [24]. The enlarged version of the (112) reflection for different concentrations of Eu^{3+}, shown in Fig. 2(c), illustrates the peak shift for varying concentration of Eu^{3+}. At 1.5 and 2.0 mol.% of Eu^{3+}, the peaks became narrow, with increased intensity and reduced widths. The narrowing of the diffraction peaks and increased intensity indicate an improvement in crystallinity. In addition, anion groups have also been reported to contribute positively tocrystallization of $CaMoO_4$[25]. The shift in the peak positions was most likely due to micro strains resulting from the incorporation of Eu^{3+} and SO_4^{2-}. The average crystallite size (*D*) of the $CaMoO_4$ and $CaMoO_4$-SO_4:*x*Eu^{3+} phosphors were calculated for the prominent (112) XRD peak using Scherrer's formula [26]. The average crystallite size of $CaMoO_4$ was ~ 46 nm, the sizes of Eu^{3+} doped $CaMoO_4$-SO_4 phosphors increased from ~50 nm to ~70 nm, and the FWHM of the diffraction peak decreased with increasing Eu^{3+}concentration as shown in Fig. 2(c).

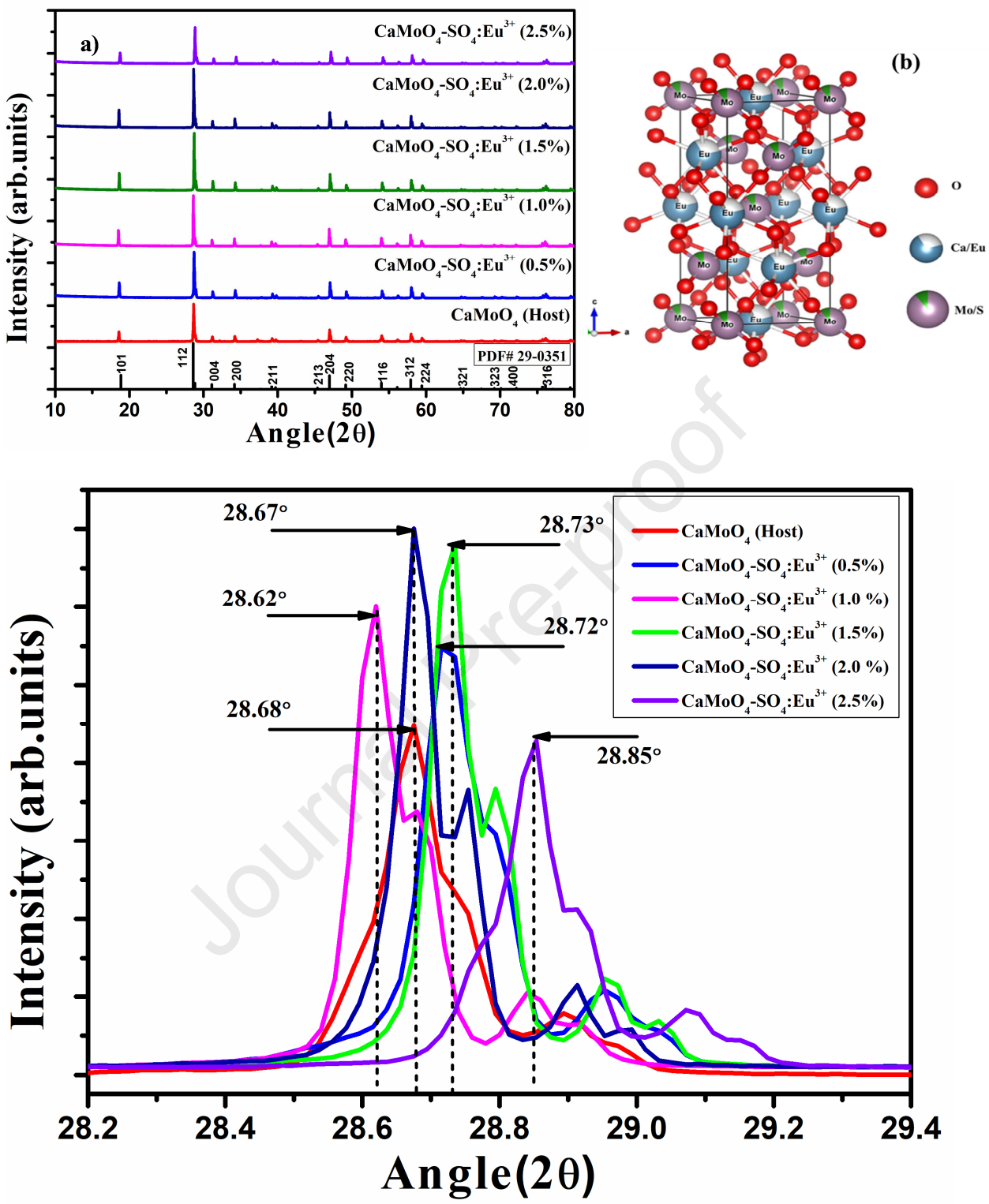

Fig.2: *(a) X-ray diffraction patterns of $CaMoO_4$ and $CaMoO_4$-SO_4:xEu^{3+} phosphors and (b) crystal structure of $CaMoO_4$-SO_4:Eu^{3+} and (c) magnified view of the (112) diffraction peak.*

3.2 Particle Morphology and Chemical composition analyses:

Fig 3(a) shows the EDS spectrum of $CaMoO_4$-SO_4:Eu^{3+} confirming the presence of all the elements including Mo, O, Ca, S and Eu and the inset, Fig 3(b), shows the weight

percentages of these elements. The weight percentage of Mo is greater than that of O, Ca, Eu and S. Fig. 3(c) shows the SEM image of the $CaMoO_4$-SO_4:(1 mol%) Eu^{3+} powder phosphor The powder was made of irregularly shaped particles agglomerated together, with different sizes and well-defined grain boundaries. The need for prolonged heat treatment in the solid-state route leads to aggressive grain growth and agglomeration, thus forming large micrometric particles [27].

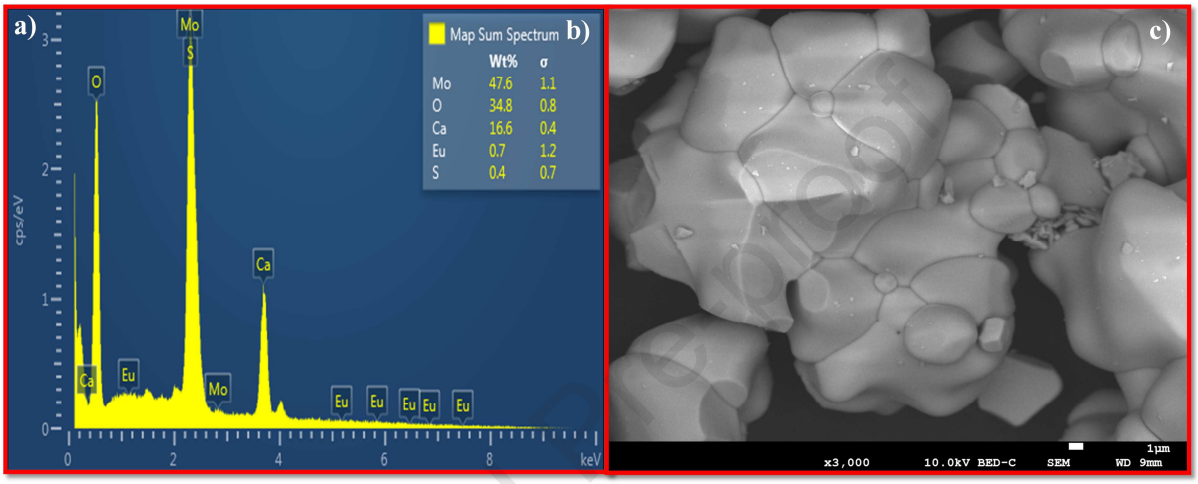

Fig. 3: *(a) EDS spectra of $CaMoO_4$-SO_4:Eu^{3+} phosphor b) Map sum spectra and (c) SEM image showing the morphology.*

3.3 Fourier-transformation infrared analysis:

The FT-IR spectra of the $CaMoO_4$, $CaMoO_4$:Eu^{3+} and $CaMoO_4$-SO_4:Eu^{3+} phosphors are displayed in Fig. 4 (a). All the spectra have a broad band around 1131 cm^{-1} which is attributed to O-H-O absorption. Weak absorption peaks at 1798 and 2409 cm^{-1} are ascribed to the vibrational bending of O-H bonds, resulting from atmospheric moisture absorbed on the surface. The bands at 911 and 811$cm^{-1}$are attributed to stretching vibration of O-Mo-O in MoO_4^{2-}[28]. Weak broad vibration peaks around 1128, 1041 and 1005 cm^{-1} are due to SO_4^{2-} pointing to successful incorporation of SO_4 in the host lattice [29]. The absorption bands around 424 and 475 cm^{-1} are associated with the bending vibration of Mo-O groups. Fig. 4(b) showed the schematic diagram of the bending and stretching vibrations of MoO_4 and SO_4.

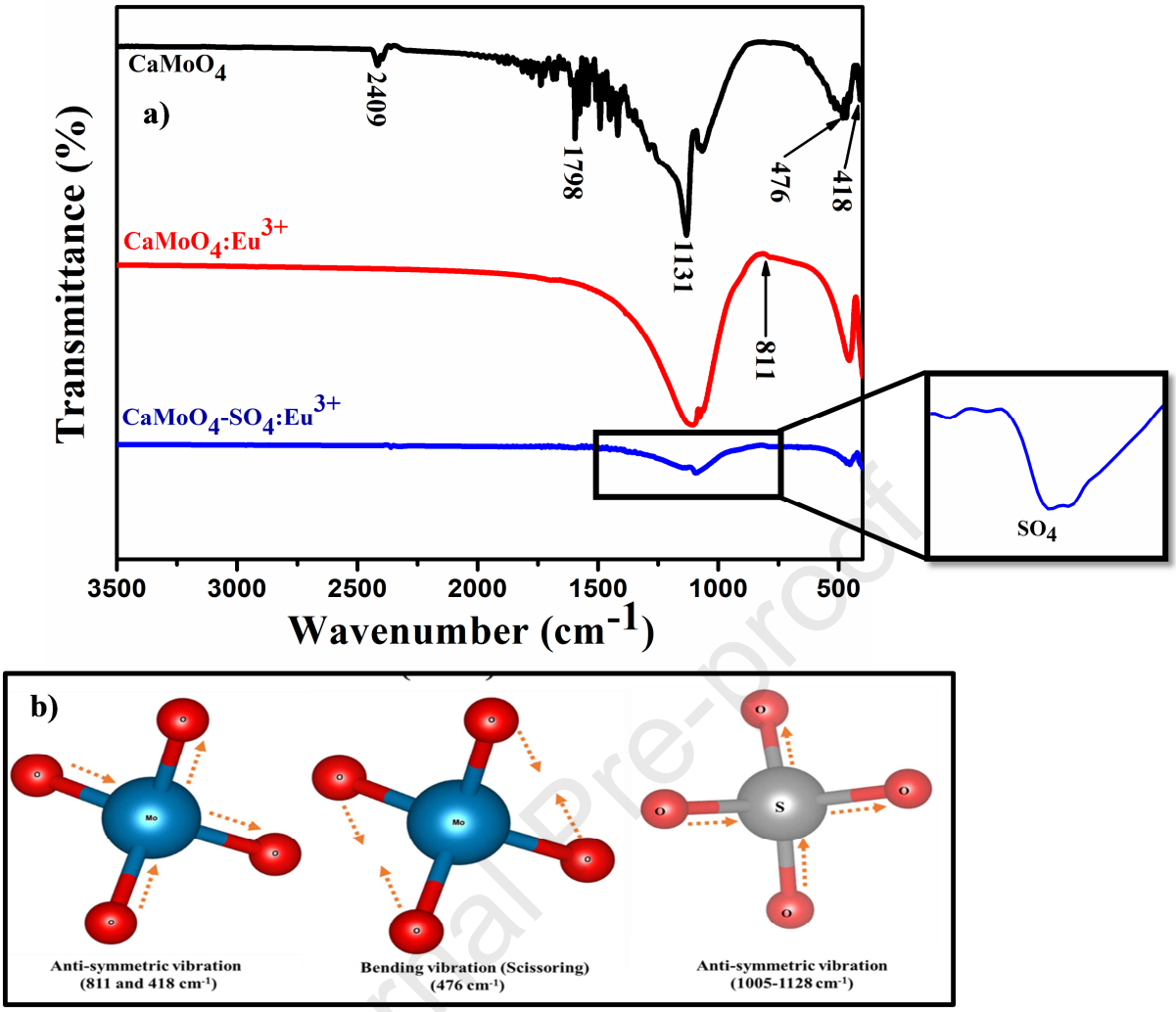

Fig. 4 (a): *FTIR spectrum of $CaMoO_4$:Eu^{3+} 1.0 mol %, $CaMoO_4$-SO_4:Eu^{3+}1.0 mol% and* ***(b)*** *Schematic diagram of MoO_4 and SO_4 structural groups.*

3.4 X-ray Photoelectron Spectroscopy: Surface Chemical Composition analysis

The XPS survey spectrum shown in Fig. 5 displays the electronic and chemical composition of the 1.0 mol% Eu^{3+} doped $CaMoO_4$-SO_4 phosphor. All observed peaks in the spectrum confirmed the presence of Ca, Mo, O, Eu, S and C in the $CaMoO_4$-SO_4:Eu^{3+} phosphor. C was from adsorbed atmospheric hydrocarbons and/or from the carbon tape [30, 31] on which the samples were mounted. Fig. 6 (a) and (b) present the high resolution XPS spectrum of Ca before and after sputtering respectively. Before sputtering the XPS peak for the Ca (2p) has a core binding energies (BE) of 350.8 eV and 347.2 eV for the $2p_{1/2}$ and $2p_{3/2}$, respectively. These peaks have the FWHM of 3.0 and 2.5 eV, respectively, for the $2p_{1/2}$ and $2p_{3/2}$ doublets. These results show that the Ca oxidation state was stabilized into the +2 state. The XPS spectrum in Fig. 7 (a) shows the high resolution peaks of the Mo 3d with the

FWHM of 1.8 for the $3d_{5/2}$ and 1.8 eV for the $3d_{3/2}$ with the core BE of 233.3 eV and 235.5 eV respectively, consistent with similar peaks reported previously[30]. There is a significant change in the FWHM, peak positions, and intensity of the Mo 3d spectrum after sputtering as shown in Fig.7(b). Mo (3d) XPS peaks illustrates the BE shift of $3d_{3/2}$ for 2.1 eV and $3d_{5/2}$ for 1.4eV with the corresponding FWHM of 4.8 eV and 1.0 eV. A minor peak was observed at 229.2 eV, which is associated with the lower oxidation state or the Mo metallic peak for the Mo 3d [31]. Fig 8 shows the high resolution XPS spectra of O1s (a) before and (b) after sputerring. The spectra were fitted with three- peaks using a multipack software. The peaks are labelled O_1 (532.1eV) O_2 (530.4 eV) and O_3 (529.8eV) and they are respectively assigned to chemisorbed oxygen, oxygen ion vacancies in the lattice and adsorbed water molecules on the surface of the $CaMoO_4$-SO_4:Eu^{3+} phosphor [32-34]. After sputtering, the O_2peak became less intense and shifted to the higher binding energy side. The high resolution XPS spectrum for S 2p core-level shown in Fig. 9(a) consists of two peaks located at 162.1 and 166.5eV and they are attributed to the S $2p_{3/2}$ and S $2p_{1/2}$, respectively[35, 36]. The S 2p peak is acribedto S in the SO_4 ions as reported previously [37]. The high resolution XPS spectrum of the Eu3dis shown in Fig.9 (b). The high-signal-to-noise-ratio is due to relatively lower concentration levels of Eu^{3+}[38]. The peak around 1135 eV corresponds to $Eu^{3+}3d_{5/2}$ while the peak at 1165 eV corresponds to Eu^{3+} $3d_{3/2}$ and these peaks are consistent with the reported values for the +3 oxidation states of the Eu ions [39]

Journal Pre-proof

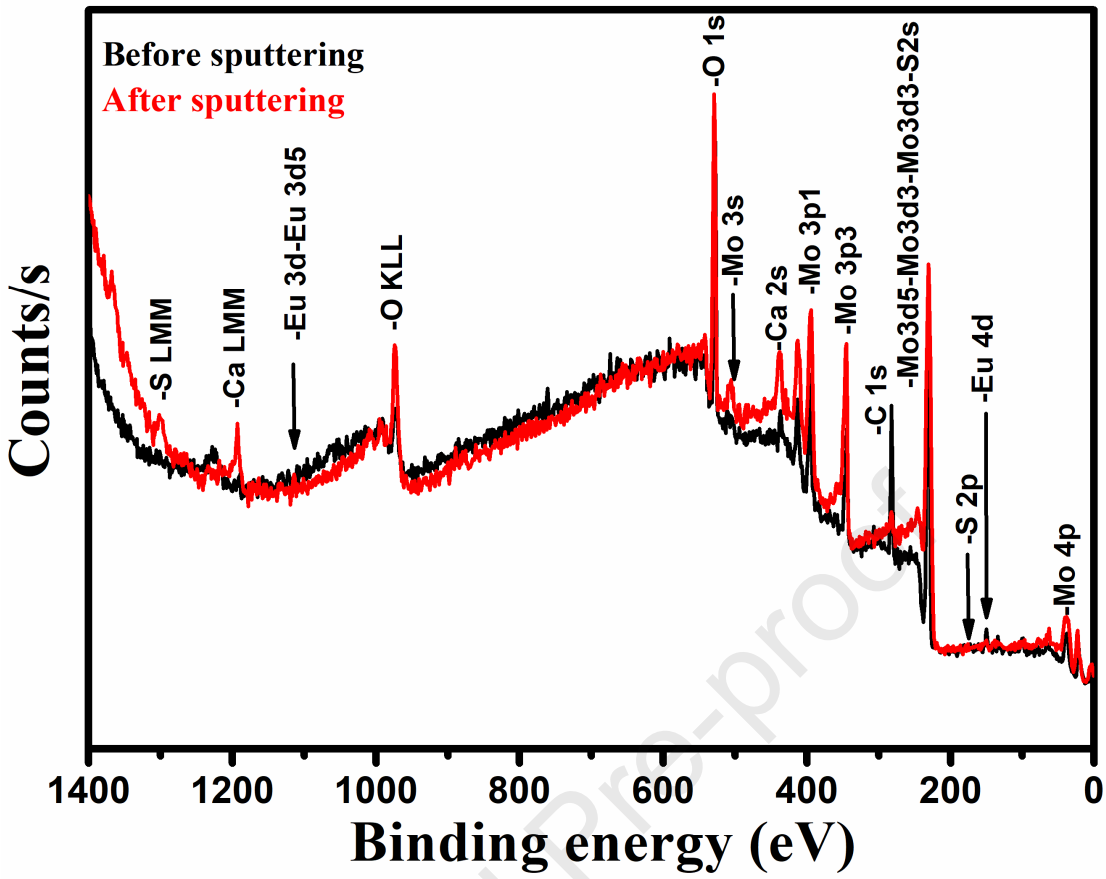

Fig. 5: *XPS spectra of the $CaMoO_4$-SO_4:$Eu3^+$ phosphor before and after sputtering.*

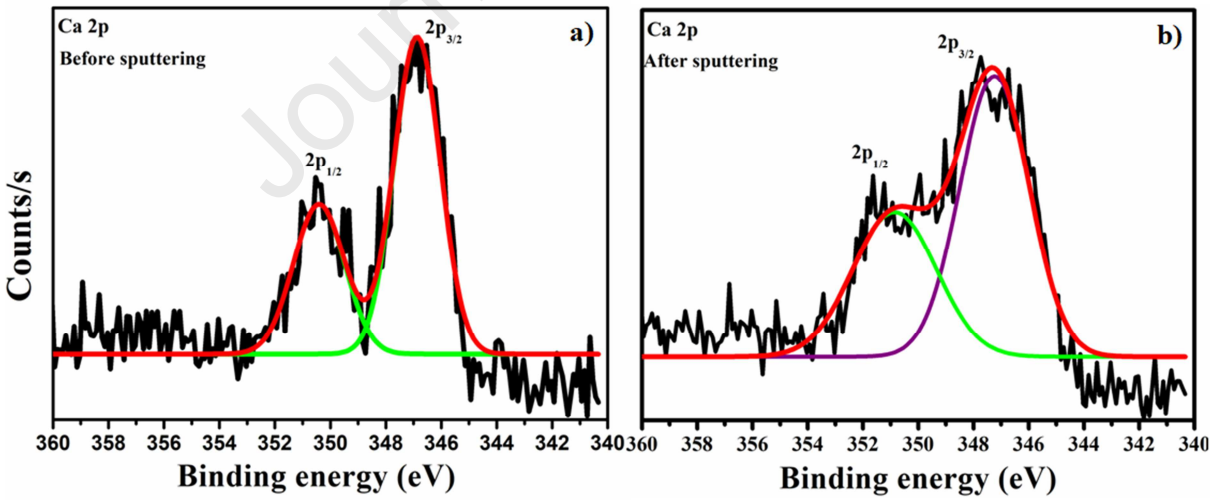

Fig. 6: *(a) XPS Spectra of Ca 2p before and (b) after sputtering.*

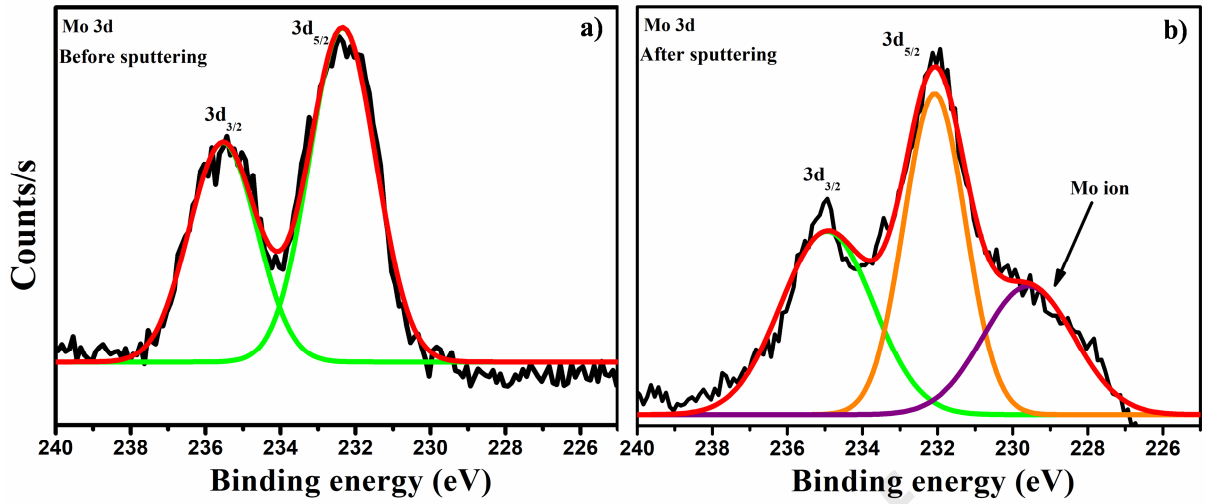

Fig. 7: *(a) XPS spectra of Mo 3d before and (b) after sputtering.*

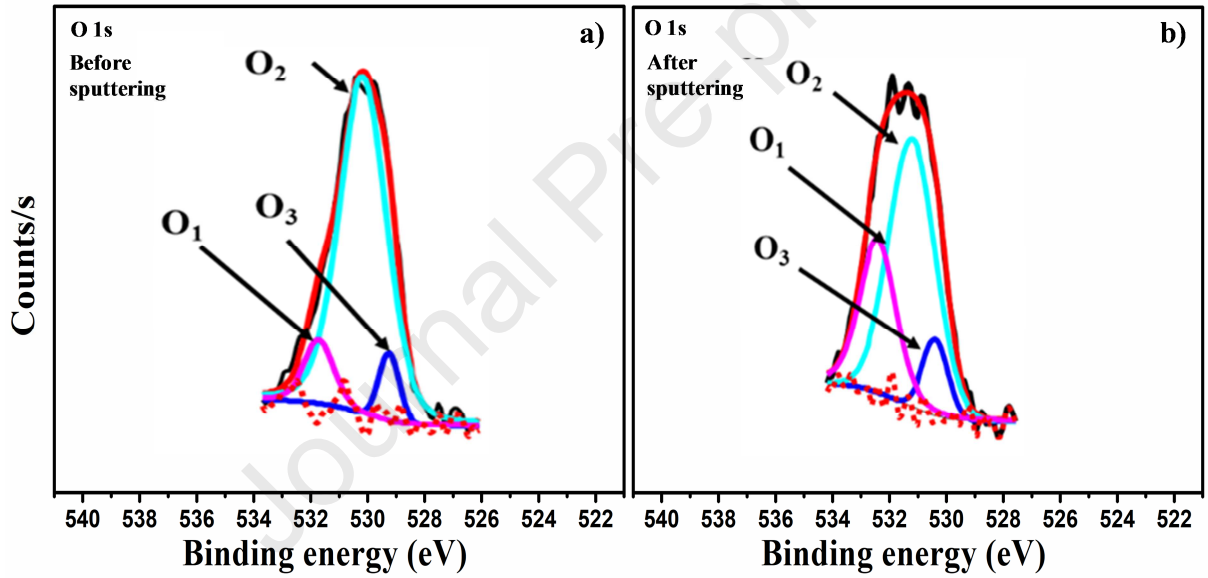

Fig. 8: *The high resolution XPS scan spectrum of O 1s of $CaMoO_4$-SO_4:Eu^{3+}(1.0 mol % of Eu^{3+}) before and after sputtering.*

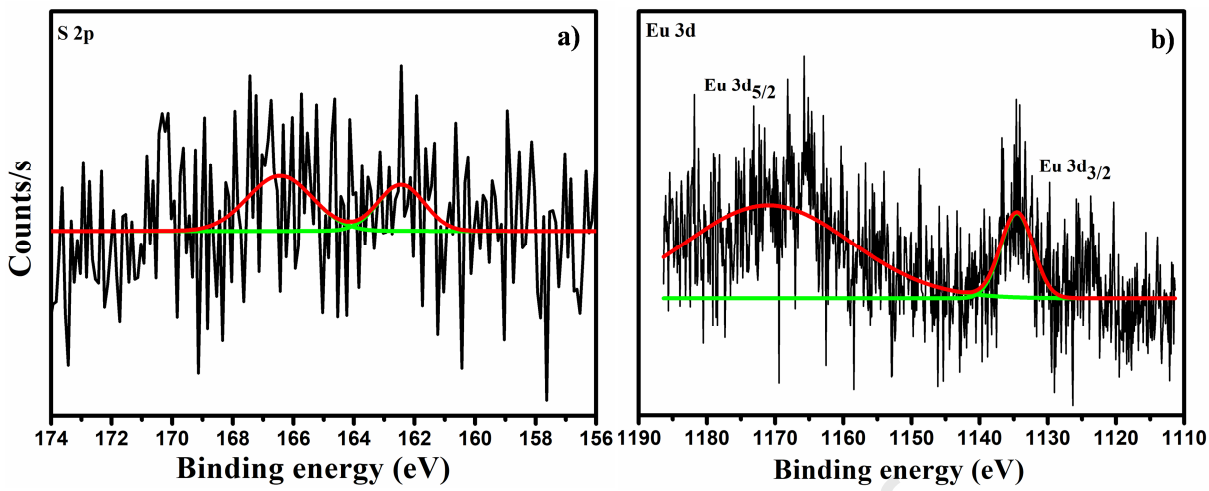

Fig. 9 *The high resolution XPS scan spectra of* ***(a)****S 2p and* ***(b)****Eu3d for of $CaMoO_4$-SO_4:Eu^{3+}(1.0 mol %) phosphors.*

3.4 Ultraviolet-visible absorption spectroscopy:

Fig.10 shows the optical diffuse reflectance spectra (DRS) of the $CaMoO_4$host and $CaMoO_4$-SO_4:xEu^{3+} (x = 0.5, 1.0, 1.5, 2.0 and 2.5 mol. %). All the DRS spectra of $CaMoO_4$ host and $CaMoO_4$-SO_4:xEu^{3+} showed similar pattern except additional absorption bands from $CaMoO_4$-SO_4:xEu^{3+} which are attributed to the f-f absorptions of Eu^{3+} dopants. The absorption of the $CaMoO_4$ host is located at ~450 nm, which has been associated with the O^{2-} →Mo^{6+}charge transfer absorption band [40]. This indicates that our phosphors were capable of absorbing in the near ultraviolet region efficiently. This broad absorption peak wavelengths shifted towards the shorter wavelengths with increasing Eu^{3+} concentration. Other than the MoO_6^{6-} group absorption band, additional absorption bands attributed to the typical *f-f* transitions of the Eu^{3+} ion were detected at 457, 535, 1385, 1962, 2061 and 2200 nm. The optical band gap of the $CaMoO_4$ and $CaMoO_4$-SO_4:xEu^{3+}(x = 0.5, 1.0, 1.5, 2.0 and 2.5 mol.%) phosphor materials were calculated by using the Kubelka–Munk function (R) as shown in Fig. 11[41]. The optical band gap for these $CaMoO_4$, and $CaMoO_4$-SO_4 doped with 0.5, 1.0, 1.5, 2.0 and 2.5 mol% of Eu^{3+} were found to be 3.72, 4.66, 4.60, 4.34, 4.30 and 4.57 eV respectively. The increased bandgap were found in Eu^{3+} doped $CaMoO_4$-SO_4 phosphors and this attributed to incorporation of Eu^{3+} and SO_4^{2-} ions. As can be seen in Fig. 8, the energy band gap values were progressively suppressed with increasing Eu^{3+}concentration. The variation in optical band gap energy values are associated with the changes in the local atomic structure or lattice. These band gap values were greater than those reported previously [42, 43].

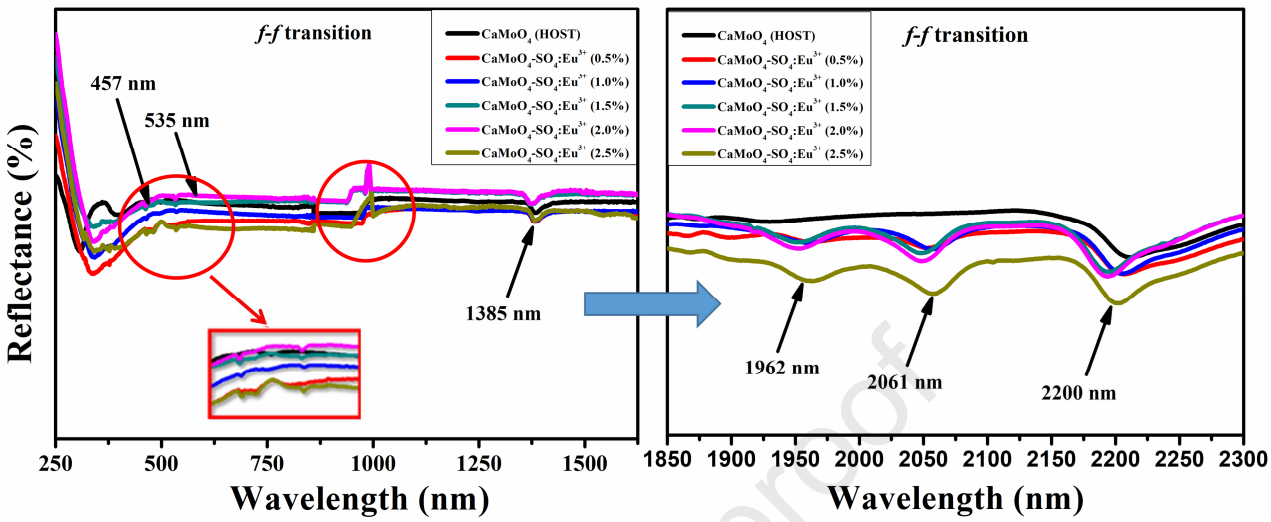

Fig.10: *Diffuse reflection spectra for $CaMoO_4$-SO_4:xEu^{3+}* (*x* = 0.5, 1.0, 1.5, 2.0 and 2.5 mol. %) *phosphor materials.*

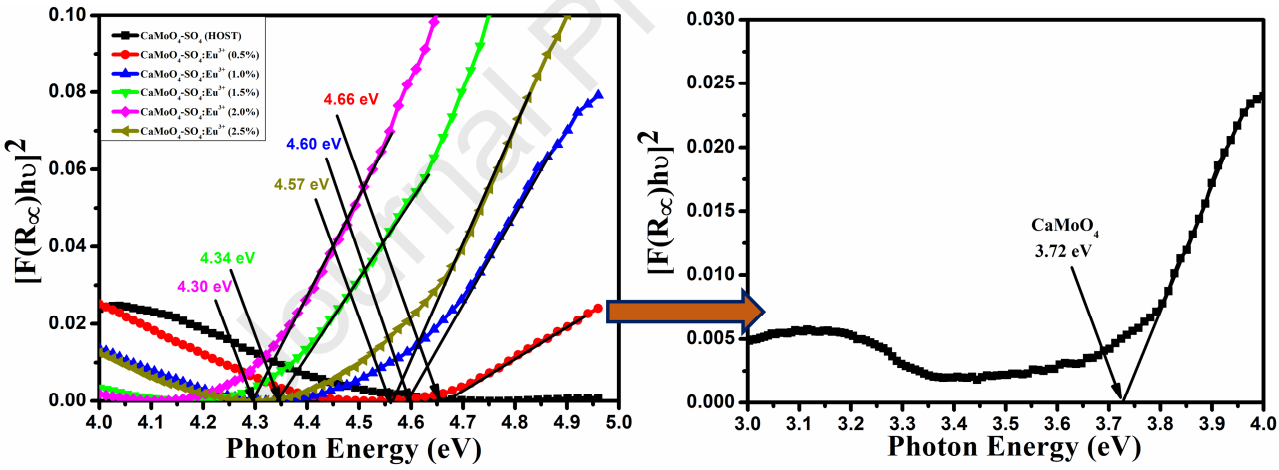

Fig.11: *Optical band gap determination of the $CaMoO_4$-SO_4:xEu^{3+}*(x = 0.5, 1.0, 1.5, 2.0 and 2.5 mol. %) *phosphor materials.*

3.5 Photoluminescence properties of $CaMoO_4$-SO_4:Eu^{3+}

Fig.12 shows the PL excitation spectra of the $CaMoO_4$ host and the $CaMoO_4$-SO_4:xEu^{3+} (x = 0.5, 1.0, 1.5, 2.0 and 2.5 mol. %) phosphors recorded when monitoring the emission peak of Eu^{3+} ($^5D_0 \rightarrow {}^7F_2$) at the wavelength of 615 nm. The excitation peaks located at 361, 382, 395 and 416 nm correspond to the $^7F_0 \rightarrow {}^5G_4$, $^7F_0 \rightarrow {}^5G_2$, $^7F_0 \rightarrow {}^5L_6$ and $^7F_0 \rightarrow {}^5D_3$ transitions of Eu^{3+} ions, respectively. Under excitation at 395 nm, the emission spectra of $CaMoO_4$-SO_4:xEu^{3+} (x = 0.5, 1.0, 1.5, 2.0 and 2.5 mol. %) phosphors were recorded and are shown in Fig. 13. The

emission peaks at 575 nm and 750 nm are due to the $^5D_0 \rightarrow {}^7F_J$ (J = 1, 2, 3, 4) transitions of Eu^{3+} ions, respectively. The strongest emission peak at 615 nm is due to the $^5D_0 \rightarrow {}^7F_2$ transitions of Eu^{3+}.The weak emissions located at 592, 655 and 702 nm, are associated, respectively, with the $^5D_0 \rightarrow {}^7F_1$, $^5D_0 \rightarrow {}^7F_3$ and $^5D_0 \rightarrow {}^7F_4$, transitions of Eu^{3+}[44]. The $^5D_0 \rightarrow {}^7F_2$ transition is associated with the electric dipole, that is insensitive to the lattice site symmetry of the Eu^{3+} ions. The $^5D_0 \rightarrow {}^7F_2$ transition is much stronger than the $^5D_0 \rightarrow {}^7F_1$ transition, indicating that the Eu^{3+} ion is placed in a distorted local environment [45]. Partially substituting Ti with SiO_2 reduced the density of defects and improve the crystal surroundings of Pr^{3+} which resulted in the increase of the rate of energy transfer from the $CaTiO_2$ to Pr^{3+}, and a subsequent increase in emission intensity from Pr^{3+} [46]. In this study, the same behavior was observed where the substitution of SO_4^{2-} anions and the defect densities were reduced as non-radiative centres and improved the local distortion of the crystal field surrounding the Eu^{3+}in $CaMoO_4$ during calcination. This phenomenon has tendency to increase the rate of energy transfer from the $CaMoO_4$hostto Eu^{3+} ions. In addition, the SO_4^{2-} ion act as charge compensator or sensitizer [47]. Fig.14 (a) shows the PL maximum intensities of the $CaMoO_4$-SO_4:$x$$Eu^{3+}$ phosphor material as a function of different Eu^{3+} ion concentrations for the major emission peak associated with the $^5D_0 \rightarrow {}^7F_2$ transition. The PL intensity increased with increasing Eu^{3+} ion concentration from 0 mol%, maximized at 1.0 mol% and then decreased when the concentration was increased to 2.5 mol.%. The decrease of the PL intensity at Eu^{3+} concentrations above1.0 mol% is ascribed to concentration quenching effect [48]. By using the Van Uitert equation (5), the interaction type responsible for the energy transfer was determined [49].

$$\frac{I}{x} = \frac{k}{(1+\beta(x)^{\theta/3})}, \tag{5}$$

where I/x is the emission intensity per ion concentration (x), β and k are the constants for a given host lattice, and θ is a function of multipole-multipole interaction. When the values of θ are 6, 8, and 10, it shows respectively the d–d (dipole-dipole), d–q (dipole-quadrupole), and q–q (quadrupole-quadrupole) interactions. Fig. 14(b) shows a graph of the *I/x* versus x (where I is the emission intensity and x is the doping concentration) on the logarithmic scale. The graph is of a linear type with a slope of -2.024, which is equal to $-\theta/3$. Therefore, the value of θ is ~6, suggesting that the d–d is the type of interation responsible for the quenching effect of the PL emission of Eu^{3+} ions in the $CaMoO_4$-SO_4 phosphors.

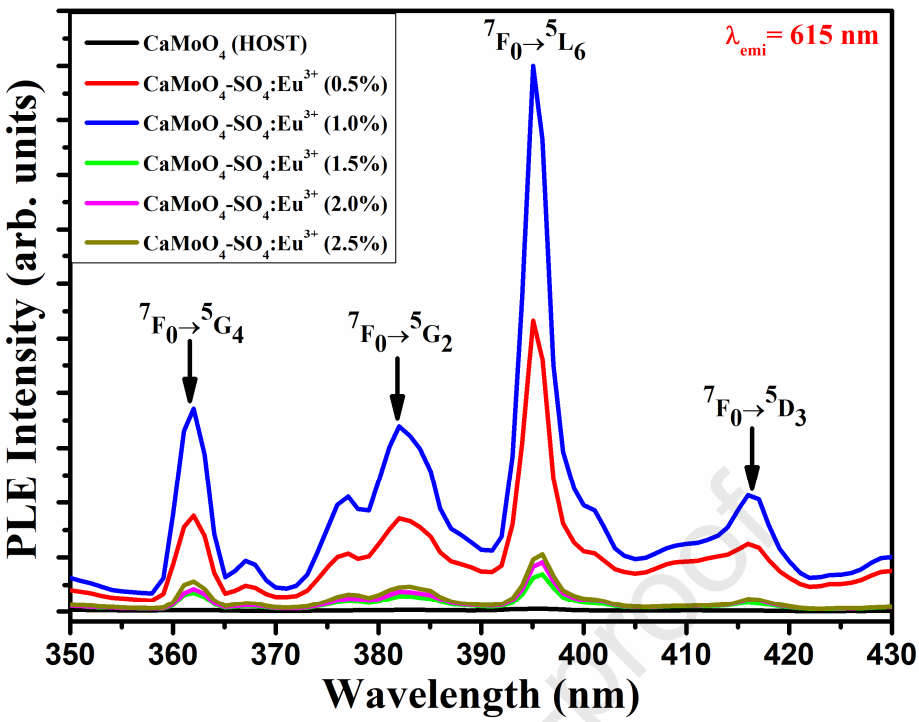

Fig. 12: *PL excitation spectra of $CaMoO_4$-SO_4:xEu^{3+} (x = 0.5, 1.0, 1.5, 2.0 and 2.5mol. %) monitored under 615 nm emission wavelength.*

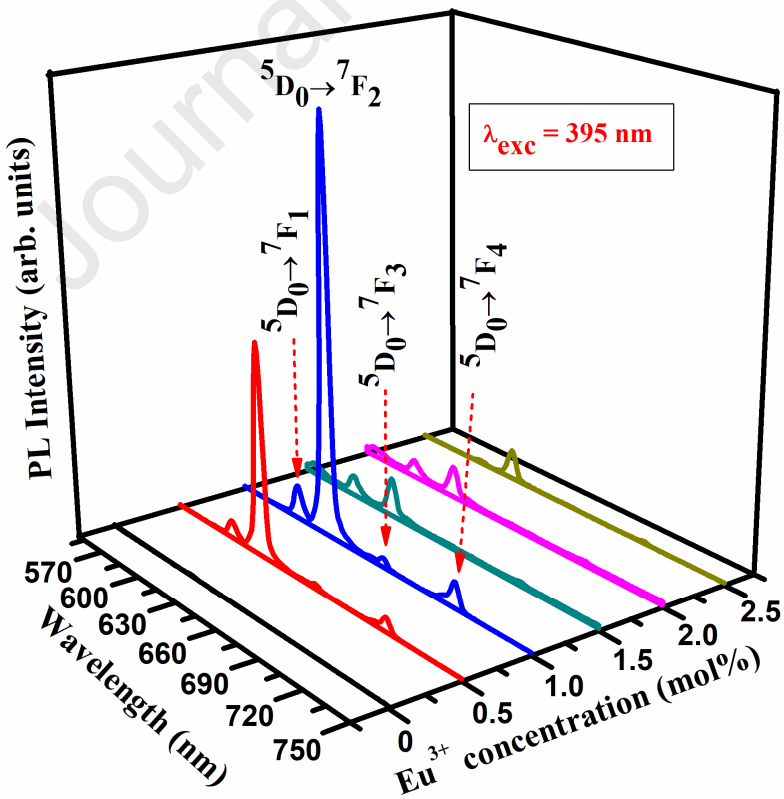

Fig. 13: *PL emission spectra of $CaMoO_4$-SO_4:Eu^{3+} x mol%. (x = 0.5, 1.0, 1.5 2.0 and 2.5) monitored under 395 nm excitation wavelength.*

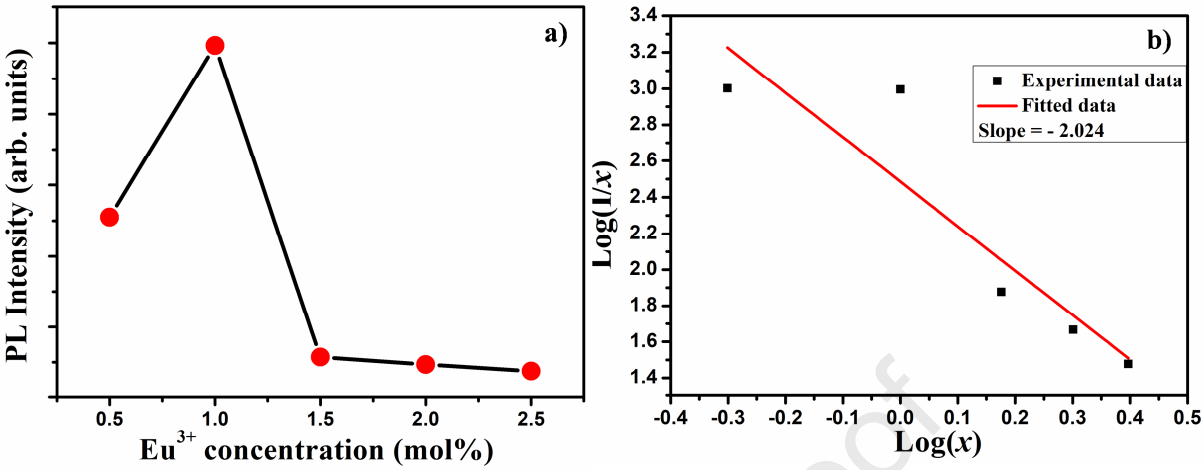

Fig. 14: *(a) Photoluminescence emission intensity as a function of Eu^{3+} ion concentration and (b) Log (I/x) versus log(x) plot of $CaMoO_4$-SO_4:Eu^{3+} phosphors*

3.6. Energy transfer mechanism between MoO_4^{2-} to Eu^{3+} ion

Fig. 15 shows the schematic diagram explaining the mechanism of energy transfer from MoO_4^{2-} to the 4*f* ground level of Eu^{3+}. A similar mechanism was proposed by Lee et al.[50]. Under UV excitation, the host electrons make a transition from the $^1A_1$ ground state to the $^1T_1$ excited state. When the Eu^{3+} ions are incorporated in the $CaMoO_4$-SO_4, the energy is transferred from MoO_4^{2-} to the unexcited 4*f* levels of the Eu^{3+} ions. Therefore, an electron may relax non-radiactively as it makes a transition from the higher excited energy states to the lower energy states and multiple photon emission occur during this transition. This absorbed primary energy is transferred from the MoO_4^{2-} to the Eu^{3+} ion, resulting in the electronic transition from the $^7F_0$ ground state to the $^5L_6$ excited states of the Eu^{3+} ion. The $^5L_6$, and ^5D_j (j= 1, 2, 3) levels decays non-radioactively to the $^5D_0$ level followed by the radiative emission of visible photons during a transition from the $^5D_0$ to ^7F_J (J=1, 2, 3, 4) levels of Eu^{3+} ions.

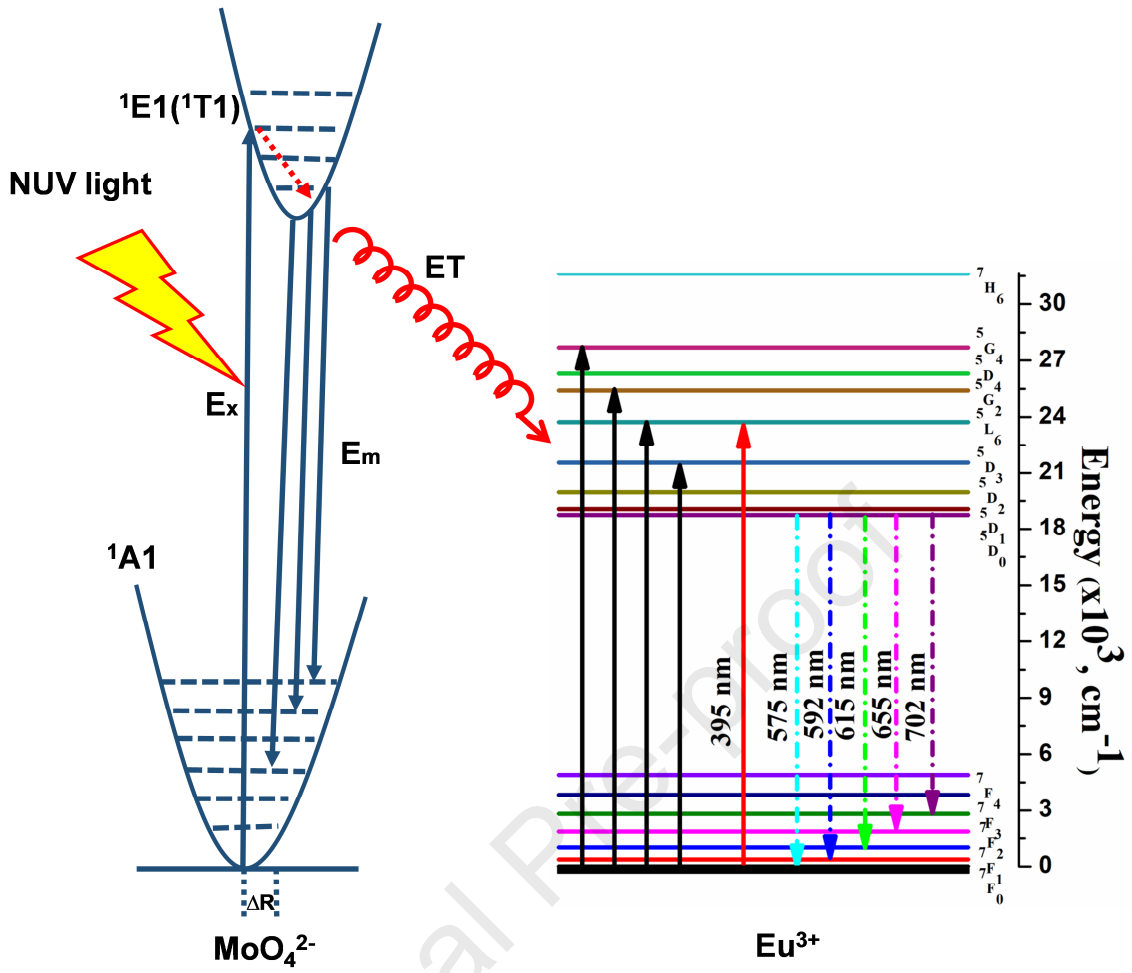

Fig. 15: *The energy level diagram and the energy transfer process in $CaMoO_4$-SO_4: Eu^{3+} phosphor.*

3.7. Phosphorescence decay time curves:

Fig. 16 depicts the decay behaviour of the $^5D_0 \rightarrow {}^7F_2$ transition emission line for Eu^{3+} in the $CaMoO_4$:Eu^{3+} and the $CaMoO_4$-SO_4:Eu^{3+} samples. The experimental curves were fitted using a double-exponential function:

$$I(t) = A_1 \exp\left(-\frac{t}{\tau_1}\right) + A_2 \exp\left(-\frac{t}{\tau_2}\right), \quad (6)$$

where *I(t)* is the phosphorescence intensity, A_1 and A_2 are the constants, and τ_1 and τ_2 are the lifetimes or decay constants. The lifetime of $CaMoO_4$:Eu^{3+} is 430 ms, while that $CaMoO_4$-SO_4:Eu^{3+} is 442 ms (i.e. 12 ms longer than the former). These results provides direct evidence that SO_4^{2-} does have a positive effect on the PL intensity and lifetime of $CaMoO_4$:Eu^{3+} material. It is therefore reasonable to conclude that SO_4^{2-}ions acted toharvest and transfer

primary excitation energy to Eu^{3+} resulting in improved red photoluminescence of Eu^{3+} at the wavelength of 625 nm.

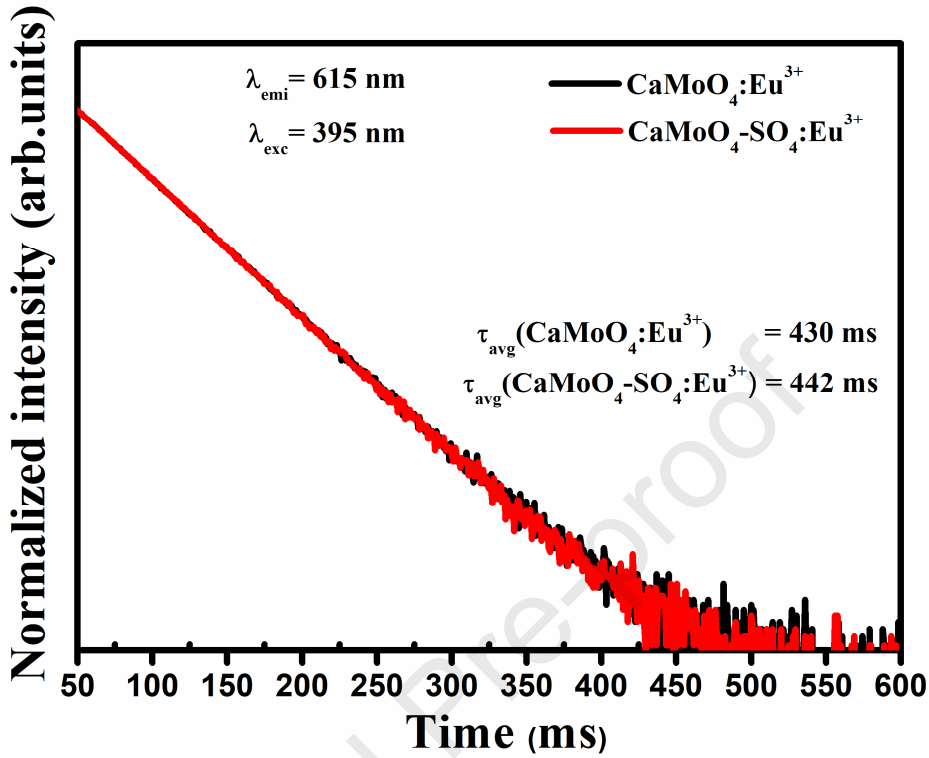

Fig. 16: *The fluorescence decay curves of $CaMoO_4:Eu^{3+}$(1mol%) and $CaMoO_4$-SO_4:Eu3$^+$(1mol%) phosphors.*

3.8. *CIE-color-coordinates and CCT of $CaMoO_4$-SO_4:Eu^{3+} phosphors:*

The CIE chromaticity coordinates diagram of $CaMoO_4$-SO_4:xEu^{3+} is shown in Fig. 17. The colour was tuned from orange-yellow to red, as we vary the molar concentration of Eu^{3+}. The CCT was determined using McCamy empirical formula: [51]

$$\mathbf{CCT} = -437n^3 + 3601n^2 + 6861n + 5514.1 \quad (7)$$

where $n = (x-x_e)/(y-y_e)$ and $x_e = 0.332$ and $y_e = 0.1858$

The CIE coordinates and the CCT values are presented in Table 1. The CIE coordinates show that our phosphors changed colour from orange-red to red colour with incorporation of the SO_4^{2-} anionic groups and different concentrations of Eu^{3+}. This confirmed that the emission colours were tunable. The CCT values of our phosphors were found in the range of 3879 K-7391 K for different Eu^{3+} ion concentrations. For the purpose of commercial lighting, the CCT value lower than 5000 K is certainly the cold red light. The obtained CCT values of $CaMoO_4$-SO_4:xEu^{3+} (x= 0.5, 1.0 and 1.5) are in close agreement with the CCT value of the at

noon (i.e. standard daylight at noon) (5000 - 5400 K) that is suitable for cold light emission [52]. The present results suggest that our materials are promising candidates for producing cool red light illumination. The colour purity is one of the important features for evaluating performance of phosphors, and it can be determined using equation (8):

$$\text{Color purity} = \frac{\sqrt{(x-x_{ee})^2+(y-y_{ee})^2}}{\sqrt{(x_d-x_{ee})^2+(y_d-y_{ee})^2}} \times 100\%, \quad (8)$$

where (x, y), (x_{ee}, y_{ee}), and (x_d, y_d) are the CIE color chromaticity coordinates of the sample point, the standard equal-energy point (0.3333, 0.3333), and the dominant-wavelength point of the sample, respectively. The color purity values of the $CaMoO_4$-SO_4:Eu^{3+}phosphorsare listed in table 1, and were found to be in the range of 89–97%, which is greater than the standard red emitting phosphor ($CaMoO_4$:Eu^{3+}). The values shown in table 1 indicate that the phosphors having a composition of the $CaMoO_4$-SO_4:xEu^{3+} (0.5 and 1 mol. %) showed the maximum red color emission and an exceptional colour chromaticity coordinates with an improved colour purity.

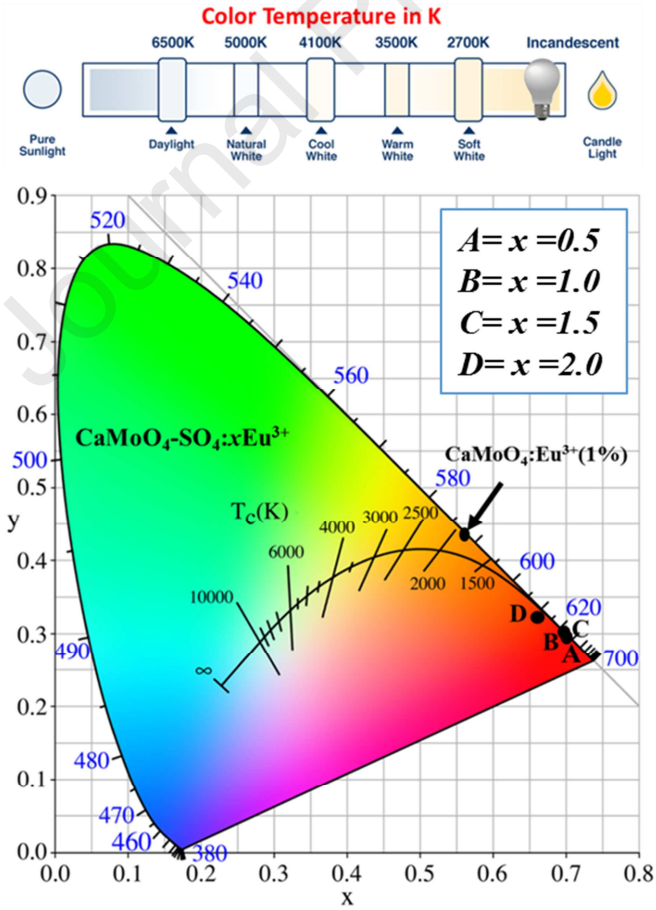

Fig. 17: *CIE chromaticity diagram of the $CaMoO_4$-SO_4: xEu^{3+} phosphors.*

Journal Pre-proof

Samples	CIE 1931 Coordinates		CCT values (K)	Colour purity (%)	Colour
	x	y			
$CaMoO_4$:1.0Eu^{3+}	0.57	0.42	1805	68	Orange-red
$CaMoO_4$-SO_4:0.5Eu^{3+}	0.69	0.31	5194	97	Red
$CaMoO_4$-SO_4:1.0Eu^{3+}	0.69	0.31	5194	97	Red
$CaMoO_4$-SO_4:1.5Eu^{3+}	0.67	0.30	7391	92	Red
$CaMoO_4$-SO_4:2.0Eu^{3+}	0.66	0.32	3879	89	Red

Table 1: *CIE1931 chromaticity coordinate, CCT and colour purity values of $CaMoO_4$-SO_4:xEu^{3+}(x = 0.5, 1.0, 1.5, 2.0, and 2.5) and the corresponding colors.*

Conclusion:

$CaMoO_4$-SO_4:xEu^{3+} (x = 0.5, 1.0, 1.5, 2.0 and 2.5 mol. %) phosphor powders were successfully synthesized by the solid-state reaction method. The structural, morphological, and optical properties were investigated using different techniques. The XRD diffraction patterns were consistent with those reported in the standard JCPDS file no. 29-351 of the pure tetragonal phase of $CaMoO_4$. The DRS absorption spectra showed that the optical absorption band gap of our phosphors shifted toward the lower energies due to incorporation of the SO_4^{2-}. The PL properties showed the tunable emission from orange-red to red emission colour that was dependent on the Eu^{3+} concentration. Incorporation of the SO_4^{2-} into the host lattice improved the emission intensity of $CaMoO_4$:Eu^{3+}, which confirms that SO_4^{2-} ions are excellent sensitizer of the red emission. The purity of the red emission was analysed and the CIE coordinates, CCT and color purity analysis results suggest that our materials are suitable for use as sources of red light in displays and light emitting devices of different types.

.

Acknowledgments

The South African National Nanoscience Postgraduate Teaching and Training Platform (NNPTTP) of the Department of Science and Technology support this work financially.OMN would like to acknowledge financial support from the Competitive Programme for Rated Researchers (CPRR) (Grant no. CPR20110724000021870) of the National Research Foundation (NRF)-South Africa. This research was also financially supported by PDRFs, Global Excellence and Stature Funding (GES) programme, University of Johannesburg and Faculty of Science, University of Johannesburg, South Africa. HCS acknowledge the Sarchi chair initiative of the Department of Science and Technology (84415) for equipment and financial support.

References

[1] Y. Liu, G. Liu, J. Wang, X. Dong, W. Yu, Single-component and warm-white-emitting phosphor $NaGd(WO_4)_2$:Tm^{3+}, Dy^{3+}, Eu^{3+}: synthesis, luminescence, energy transfer, and tunablecolor, *Inorg. Chem.* 53 (2014) 11457–11466.

[2] M.E. Foley, R.W. Meulenberg, J.R. Mcbride, G.F. Strouse, Eu^{3+}-doped ZnB_2O_4(B =Al^{3+}, Ga^{3+}) nanospinels: an efficient red phosphor, *Chem. Mater.*27 (2015) 8362–8374.

[3] X. Huang, B. Li, H. Guo, D. Chen, Molybdenum-doping-induced photoluminescence enhancement in Eu^{3+}-activated $CaWO_4$ red-emitting phosphors for white light-emitting diodes, *Dyes Pigm.*143 (2017) 86–94.

[4] S.K. Gupta, P.S. Ghosh, A.K. Yadav, N. Pathak, A. Arya, S.N. Jha, D. Bhattacharyya, R.M. Kadam, Luminescence properties of $SrZrO_3$/Tb^{3+} perovskite: host-dopant energy-transfer dynamics and local structure of Tb^{3+}, *Inorg. Chem.* 55 (2016) 1728–1740.

[5] Y. Zhai, X. Zhao, C. Liu, P. Song, X. Jing, Y. Han, J. Wang, $CaMoO_4$:Dy^{3+},Eu^{3+} phosphors: microwave synthesis, characterization, tunable luminescence properties and energy transfer mechanism, *Optik*, 164 (2018) 433-442

[6] N. Narendran, Y. Gu, J. Freyssinier, H. Yu and L. Deng, Solid-state lighting: failure analysis of white LEDs, *J. Cryst. Growth*, 268 (2004) 449-456.

[7] A. Parchur, A. Prasad, A. Ansari, S. Rai and R. Ningthoujam, Luminescence properties of Tb^{3+}-doped $CaMoO_4$ nanoparticles: annealing effect, polar medium dispersible, polymer film and core-shell formation, *Dalton Trans.*41 (2012)11032.

[8] E. Schubert, Solid-State Light Sources Getting Smart, *Science*, 308 (2005)1274-1278.

[9] J. Park, H. Jung, G. Seeta Rama Raju, B. Moon, J. Jeong and J. Kim, Tunable luminescence and energy transfer process between Tb^{3+} and Eu^{3+} in GYAG:Bi^{3+}, Tb^{3+}, Eu^{3+} phosphors, *Solid State Sci.*, 12 (2010) 719-724.

[10] H. Jang, Y. Won and D. Jeon, Improvement of the electroluminescent property of blue LED coated with highly luminescent yellow-emitting phosphors, *Applied Phys. B*, 95 (2009) 715-720.

[11] S. Wang, Q. Sun. B. Devakumar, J. Liang, L. Sun,X. Huang, Novel highly efficient and thermally stable Ca_2GdTaO_6:Eu^{3+} red-emitting phosphors with high color purity for UV/blue-excited WLEDs, *J.AlloysCompd.*804 (2019) 93-99.

[12] Y. He, M. Zhao, Y. Song, G. Zhao and X. Ai, Effect of Bi^{3+} on fluorescence properties of YPO_4:Dy^{3+} phosphors synthesized by a modified chemical co-precipitation method, *J. Lumin.*, 131 (2011) 1144-1148.

[13] M. Piatkowska, E. Tomaszewicz Synthesis, structure, and thermal stability of new scheelite-type $Pb_{(1-3x)}hxPr_{2x}(MoO_4)_{1-3x}(WO_4)_{3x}$ ceramic materials, *J Therm. Anal Calorim* 126 (2016) 111–119.

[14] Y. Liu, H. Li, S. Tang, Q. Zhou, K. Wang, H. Tang, Z. Wang, A red-emitting phosphor $K_2[MoO_2F_4]$ $H_2O:Mn^{4+}$ for warm white light-emitting diodes with a high color rendering index, *Mater. Res. Bull.*, 122(2020) 110675.

[15] F.A. Rabuffetti, S.P. Culver, L. Suescun, R.L. Brutchey, Structural disorder in $AMoO_4$(A=Ca, Sr, Ba) scheelite nanocrystals, *Inorg. Chem.* 53 (2014) 1056–1061.

[16] S.K. Gupta, M. Sahu, P.S. Ghosh, D. Tyagi, M.K. Saxena, R.M. Kadam, Energy transfer dynamics and luminescence properties of Eu^{3+} in $CaMoO_4$ and $SrMoO_4$, *Dalton Trans.* 44 (2015) 18957–18969.

[17] Y. Hatefi, N. Shahtahmasebi, A. Moghimi,andE.Attaran, Frequency-conversion properties of Eu^{3+} doped chlorophosphateglass ceramics containing $CaCl_2$nanocrystals, *J. Lumin.*131 (2011) 114-118.

[18] A. Peter, Photoluminescence Studies of $CaMoO_4$: Eu^{3+} Phosphors, *Asian J. Mater. Chem.*1 (2016) 84-86..

[19] Z. Wang, H. Liang, M. Gong and Q. Su, Novel red phosphor of Bi^{3+}, Sm^{3+} co-activated $NaEu(MoO_4)_2$, *Opt. Mater.* 29 (2007) 896-900.

[20] P. Jaffe, Eu^{2+} Luminescence in the Ternary $EuO-Al_2O_3-SiO_2$ System, *J.Electrochem. Soc.* 116(1969) 629-633.

[21] Y. Zhang, S. Shi, J. Gao and J. Zhou, Effects of SO_2^{4-} or SiO_2^{3-} Doping on the Photoluminescence of $NaEu(MoO_4)_2$ Nanophosphors for Light-Emitting Diodes, *J Nanosci.Nanotechno.*10 (2010) 2156-2160.

[22] K. Ariga and M. Aono, *Supra-materials nanoarchitectonics*. Oxford: William Andrew, 2017.

[23] E. Gürmen, E. Daniels and J. King, Crystal Structure Refinement of $SrMoO_4$, $SrWO_4$, $CaMoO_4$, and $BaWO_4$ by Neutron Diffraction, *J. Chem. Phys.* 55 (1971) 1093-1097.

[24] L.G. Van Uitert, Characterization of energy transfer interactions between rare earth ions, *J. Electrochem. Soc.* 114 (1967) 1048–1053.

[25] W. Zhang, J. Li, Y. Wang, J. Long, and K. Qiu, Synthesis and luminescence properties $(MoO_4)_{2-x}AGx:Eu^{3+}$(AG = SO_4^{2-}, BO_3^{3-}) red phosphors for white light emitting diodes, *J. AlloysCompd.*635 (2015) 16–20.

Journal Pre-proof

[26] O. Ntwaeaborwa, S. Mofokeng, V. Kumar and R. Kroon, Structural, optical and photoluminescence properties of Eu^{3+} doped ZnO nanoparticles, *Spectrochim. Acta A* 182 (2017) 42-49.

[27] A. Varma, A.S. Mukasyan, A.S. Rogachev, K.V. Manukyan, Solution combustion synthesis of nanoscale materials, *Chem. Rev.* 116 (2016,) 14493−14586.

[28] Y. Huang, L. Zhou, L. Yang and Z. Tang, Self-assembled 3D flower-like $NaY(MoO_4)_2$:Eu^{3+} microarchitectures: Hydrothermal synthesis, formation mechanismand luminescence properties, *Opt. Mater.*33 (2011) 777-782.

[29] Y. Wang, W. Zhang, J. Li, and J. Long, Effect of MoO_4^{2-} partial substitution on the optical enhancement of $LaNa(MoO_4)_{2:}$ Dy^{3+} phosphors for white light-emitting diodes, *Mater. Sci. Semicond. Process.*41 (2016) 277-281.

[30] B. Singh, A. Parchur, R. Ningthoujam, A. Ansari, P. Singh and S. Rai, Influence of Gd^{3+} co-doping on the structural property of $CaMoO_4$Eu nanoparticles, *Dalton Trans.*, 43 (2014) 4770-4778.

[31] S. Gupta, M. Sahu, P. Ghosh, D. Tyagi, M. Saxenaand R. Kadam, Energy transfer dynamics and luminescence properties of Eu^{3+} in $CaMoO_4$ and $SrMoO_4$, *Dalton Trans.*,44 (2015) 18957-18969.

[32] A. Parchur, A. Prasad, S. Rai, R. Tewari, R. Sahu, G. Okram, R. Singh and R. Ningthoujam, Observation of intermediate bands in Eu^{3+} doped YPO_4 host: Li+ ion effect and blue to pink light emitter, *AIP Advances*, 2 (2012) 032119.

[33] B. Singh, M. Maheshwary, P. Ramakrishna, S. Singh, V. Sonu, S. Singh, P. Singh, A. Bahadur, R. Singh and S. Rai, Improved photoluminescencebehavior of Eu^{3+} activated $CaMoO_4$ nanoparticles via Zn^{2+} incorporation, *RSC Advances*5 (2015) 55977-55985.

[34] R. Karthik, J. Kumar, S. Chen, T. Kokulnathan, H. Yang and V. Muthuraj, Design of novel ytterbium molybdate nanoflakes anchored carbon nanofibers: challenging sustainable catalyst for the detection and degradation of assassination weapon (Paraoxon-Ethyl), *ACS Sustain. Chem. Eng.* 6 (2018) 8615-8630.

[35] X. Wang, Q. Xiang, B. Liu, L. Wang, T. Luo, D. Chen and G. Shen, TiO_2 modified FeS nanostructures with enhanced electrochemical performance for lithium-ion batteries, *Sci. Rep.* 3 (2013).

[36] G. Tai, T. Zeng, J. Yu, J. Zhou, Y. You are, X. Wang, H. Wu, X. Sun, T. Hu and W. Guo, Fast and large-area growth of uniform MoS_2 monolayers on molybdenum foils, *Nanoscale*, 8 (2016) 2234-2241.

Journal Pre-proof

[37] A. Balakrishna, H. Swart, R. Ramaraghavulu, A. Bedyal, R. Kroon and O. Ntwaeaborwa, Structural evolution induced by substitution of designated molybdate sites (MoO_4^{-2})with different anionic groups (BO_3^{-3} , PO_4^{-3} and SO_4^{-2}) in $CaMoO_4$:Sm^{3+} phosphors-A study on colortunable luminescent properties, *J. AlloysCompd.* 727 (2017) 224-237.

[38] J. F. Moulder, W. F. Stickle, P. E. Sobel and K. D. Bomben, Handbook of X-ray photo electron spectroscopy, PerkinElmer Corporation, Eden Prairie, MN, USA, 1992.

[39] S. Gupta, M. Sahu, P. Ghosh, D. Tyagi, M. Saxena, and R. Kadam, Energy transfer dynamics and luminescence properties of Eu^{3+} in $CaMoO_4$ and $SrMoO_4$, *Dalton Trans.* 44 (2015) 18957-18969.

[40] Y. Zhai, X. Zhao, C. Liu, P. Song, X. Jing, Y. Han and J. Wang, $CaMoO_4$ Dy^{3+}, Eu^{3+} phosphors: microwave synthesis, characterization, tunable luminescence propertiesand energy transfer mechanism, *Optik*164 (2018) 433-442.

[41] H. Philipp, Optical properties of non-crystalline Si, SiO, $SiO_x$and SiO_2, *J. Phys. Chem. Solids*32 (1971) 1935-1945.

[42] S. Dutta, S. Som, A. Kunti, S. Sharma, V. Kumar, H. Swart and H. Visser, Ag^{7+} ion induced modification of morphology, optical and luminescence behavior of charge compensated $CaMoO_4$nanophosphor, *Nucl. Instrum. Meth. B* 384 (2016) 76-85.

[43] C. Bouzidi, K. Horchani-Naifer, Z. Khadraoui, H. Elhouichetand M. Ferid, Synthesis, characterization and DFT calculations of electronic and optical properties of $CaMoO_4$,*Physica B*497 (2016) 34-38.

[44] A. K. Parchura and R. S. Ningthoujam, Behaviour of electric and magnetic dipole transitions of Eu^{3+}, $^5D_0 \rightarrow {}^7F_0$ and Eu–O charge transfer band in Li^+ co-doped YPO_4:Eu^{3+}, RSC Advances 2 (2012) 10859–10868.

[45] C. Chiu, C. Liu, S. Huang and T. Chen, White-Light-Emitting Diodes Using Red-Emitting $LiEu(WO_4)_{2-x}(MoO_4)_x$ Phosphors,*J. Electrochem. Soc.* 154 (2007) J181-J184.

[46] X. Zhang, C. Cao, C. Zhang, L. Chen, J. Zhang, X.J. Wang, Improved photoluminescence and afterglow in $CaTiO_3$:Pr^{3+} with addition of nanosized SiO_2, *Physica B*406 (2011) 3891–3895.

[47] X. Zhang et al., Photoluminescence and energy storage traps in $CaTiO_3$:Pr^{3+}, *Mater. Res. Bull.* 45 (2010) 1832-1836.

[48] G. Mhlongo, M. Dhlamini, H. Swart, O. Ntwaeaborwa and K. Hillie, Dependence of photoluminescence (PL) emission intensity on Eu^{3+} and ZnO concentrations in $Y_2O_3Eu^{3+}$and$ZnO \cdot Y_2O_3Eu^{3+}$nanophosphors, *Opt. Mater.* 33 (2011) 1495-1499.

Journal Pre-proof

[49] L.G. Van Uitert, Characterization of energy transfer interactions between rare earth ions, *J. Electrochem. Soc.* 114 (1967) 1048–1053.

[50] G. Lee and S. Kang, Solid-solution red phosphors for white LEDs, *J. Lumin.* 131 (2011) 2582-2588.

[51] C.S. McCamy, Correlated color temperature as an explicit function of chromaticity coordinates, Color Res. Appl. 17 (2) (1992) 142–144.

[52] J. Han, W. Im, G. Lee and D. Jeon, Near UV-pumped yellow-emitting Eu^{2+}-doped $Na_3K(Si_{1-x}Alx)_8O_{16\pm\delta}$ phosphor for white-emitting LEDs, *J. Mater. Chem. 2*2 (2012) 8793.

Journal Pre-proof

Journal Pre-proof

- $CaMoO_4:Eu^{3+}$ phosphors substituted with SO_4^{2-} groups were prepared via solid state reaction method.
- Photoluminescence (PL)properties of $CaMoO_4:Eu^{3+}$ were improved by SO_4^{2-} ions
- The energy transfer from MoO_4^{2-} to Eu^{3+} was showed in $CaMoO_4$ host.
- $CaMoO_4$-$SO_4:Eu^{3+}$ (1 mol %) phosphor reported the strongest PL emission.
- Orange-red to red color tuneable emission has been achieved by the SO_4^{2-} substitution.
- $CaMoO_4$-$SO_4:Eu^{3+}$ are potential candidates for UV excited red emission LED applications.

Journal Pre-proof

Journal Pre-proof

Declaration of interests

(X)The authors declare that they have no known competing financialinterestsor personal relationships that could have appeared to influence the work reported in this paper.

☐The authors declare the following financial interests/personal relationships which may be considered as potential competing interests:

Journal Pre-proof